5th International Conference on Water Resources and Arid Environments (ICWRAE 5): 507-518
7-9 January 2013, Riyadh, Saudi Arabia

Geospatial Analysis for Salinity Hazard Within a Semiarid Context

[1]K.H.M. Darwish, [2]M.A. El-Bordiny and [2]A.S. Salam

[1]Arid Land Research Institute,
City of Scientific Research and Application Technology, Borg AlArab, Alex., Egypt
[2]Department Soils, Faculty of Agricultural, Ain Shams University, Cairo, Egypt

Abstract: Salt concentration in soil has a drastic negative impact on crop growth, which results in reduced crop yield. Thus, detection and mapping saline soils is the first task before any reclamation effort can be conducted. In this research, an approach for detecting salt-affected soils in the southern part of El-Hussinia Plain, El-Sharkaiya Governorate, Egypt. The selected study area represented a good example of salt-affected area. Nevertheless, it is considered as a promising area for both agricultural expansion and urban development. The goal of the study was to characterize the geospatial distribution of the soil parameters using geostatistical technique. Specifically, it aimed to assess and map soil salinity to produce a management strategy, which is based on the spatial variability of selected soil parameters such as salt electrical conductivity, pH, SAR, ESP, $CaCO_3$, organic matter and soil texture. The longitudinal slope was also measured. The output results were used to generate geo-referenced salinity maps. The study showed that it is possible to map soil salinity variability in both discrete and continuous models, using geopedologic data and an appropriate interpolation technique. The study demonstrated the possibility of assessing and delineating the geospatial salinity distribution using distinguished soil components and survey. The Linear Spectral technique was applied in this study to improve the prediction of soil salinity with a maximum reliability of 69%. A moderate correlation was found between electrical conductivity and the spectral indices. An improvement was occured for most of the correlations after applying the Linear Spectral method. To generate a predicted salinity map, a multiple linear regression, based on the best correlated indices was conducted. The standard error of the estimate was about 12.1µS/cm.

Key words: Salt-affected soil · Remote Sensing · Salinity indicators · Spatial variability

INTRODUCTION

In order to improve the country self-supply with food and to relief larger towns from the nutrition-related consequences of a continuous increase of population, Egypt extends its agricultural land along El-Salam Canal in North Sinai. In this region, El-Salam Canal Project supplies about 168,000 hectares with mixed water from Nile mixed with agricultural drainage water to reclaim and cultivate these soils. El-Salam Canal is one of the largest drainage water reuse projects in Egypt. El-Salam Canal originates from Nile at km 219 on Domietta Branch and runs towards Suez Canal for about 89.4 km before it goes to Sinai Peninsula through an underneath siphon. About 1.9 and 0.4 milliard m^3 will be discharged from Hadous and El-Serw drains into El-Salam canal, respectively, when the canal comes into full operation within the next few years.

The first stage of the project aims at reclamation of 220,000 feddans *(feddan = 4200 m^2)* located west of the Suez Canal, while in the second stage 400,000 feddans will be reclaimed to the east side, in Sinai Peninsula [1]. Major activities in the area are running in relation to the installation of eastern irrigation commands of El-Salam Canal. Projects of fisheries and reclamation of saline soils dominate in the area.

In this research, the study area is located at El-Hussinia Plain, south of El-Salam Canal and east of El-Salam siphon. In El-Hussinia Plain, soil salinity appears to be a major threat to agricultural production. It is found that the main unsuitability criteria restricting more extend of additional areas for cultivation is the excess of salts. The agricultural development in the area is facing human-induced degradation of mainly water logging and salinity problems, due to unsustainable agricultural

Corresponding Auhtor: Arid Land Research Institute, City of Scientific Research and Application Technology, Borg AlArab, Alex., Egypt. E-mail: kdarwish@hotmail.com.

practices. Those are due to seepage from irrigation canals, inadequate drainage systems, conversion of pressurized irrigation system to surface-flooding, direct use of low quality drainage water in irrigation and mixing drainage and wastewater with irrigation water system. In addition, lack of field experience and training in managing the reclaimed agricultural areas increased the existing implementation of degradation problems. Optimizing spatial sampling scheme to reduce sampling density and estimation of unsampling values can save time and costs [2, 3]. However, its effectiveness relies on the accuracy of the spatial interpolation used to define the spatial variability.

Multivariate techniques such as geostatistics have been widely used as estimation tools. Geostatistical methods provide a means to study the heterogeneous nature of spatial distributions of soil salinity. Geostatistics provides descriptive tools such as kriging to directly implements the prediction of an attribute at an unsampled location according to known data points within a local neighborhood surrounding [4]. Many comparisons of various in-terpolation techniques have been made in respect to different data sets used, different mathematical procedures and different input parameters [5, 6]. The structure of variability in soil properties showed differences according to sampling spacing, soil properties and method used in the study [7]. Sokoti *et al*. [8] used different geostatistical methods in order to predict the soil salinity distribution in Urmia plain, Iran. They found that kriging method with gaussian model has higher accuracy for estimating of salinity levels in areas without any information. Darwish *et al*. [9] estimated spatial variability of soil salinity in Bahariya oasis, Egypt, using cokriging geostatistical algorithm method and the imagery of ETM sensor as a secondary variable. He showed the relative advantage of geostatistical methods for estimation of soil spatial data.

In order to investigate soil salinity variability in an efficient way, a step-wise approach is proposed using field data in terms of ECe measurements, remote sensing data, geopedologic legend and an appropriate interpolation technique. Hence, the main object of this study is to delineate and map salinity state in south El-Hussinia Plain, where it appears to be a major threat for agricultural production. The purpose was to check on the reliability of discrete (geopedologic survey) and continuous (by means of interpolation) models pronounced by geostatistic kriging algorithm in representing soil salinity distribution.

It will be important for soil management and enhancement of crop yield to study the spatial variability of soil salinity measurements, to draw the precise map with soil information [10, 11, 12, 13] especially for carrying out precision agricultural investigations in the future.

MATERIAL AND METHODS

General Situation of Experimental Area: For this research, a study area was selected in the southern part of El-Hussinia Plain and covering an area of about 141.6 km^2. It lies between latitudes 30° 50' – 31° 20' N and longitudes 32° 00' - 32° 30' E (Fig. 1). It is located within El-Hussinia district and extended North up till Lake Manzala, East till Bahr El-Bakar drainage line and West towards El-Dakahlia Governorate (Mataria and Manzala). Huge areas of Lake Manzala bottom have been artificially dried to expose the fluvio-marine deposits. Such deposits have a heavy clay texture with young sediment origin. These young deposits resulted from the deposition of the suspended matter by the Nile into the foreshore lakes that are directly in connection with the sea. The young fluvio-marine deposits are covered with aeolian sand and loose-like deposits in stratified layers [14].

Climate type of the investigated area is typically Mediterranean. It belongs to the arid province that characterized by a short dry period [15]. The annual average temperature is 13.8°C and average relative humidity is 75.5. The annual rainfall ranges between 63.6 and 102 mm. The wind velocity ranges between 4.5 and 7.0 km/hr. The evaporation rate attains its highest value in June (7.3 mm/day) and its lowest value in January (3.5 mm/day).

The field work was carried out to indentify the land types available. Based on the pre-field and information obtained, Twenty six soil profiles were observed and described to cover geopedological variations of the study area. Some other proposed soil observations and augers were added at the edge of the study areas to reduce the error of missing information.

The exact locations of the soil profiles and auger observation points were defined in the field using the GPS and located preciously on Fig. 1. It shows locations of the observation sites where soil samples were taken. Soil salinity (ECe dS/cm) was determined in the water extract of the saturated soil paste. The numbers of observations were determined mainly by the inherent variability of the mapping units. Detailed morphological description were recorded for each of the studied soil profiles, on the bases outlined by guideline for soil description [16] and classified according to USDA Soil Taxonomy [17].

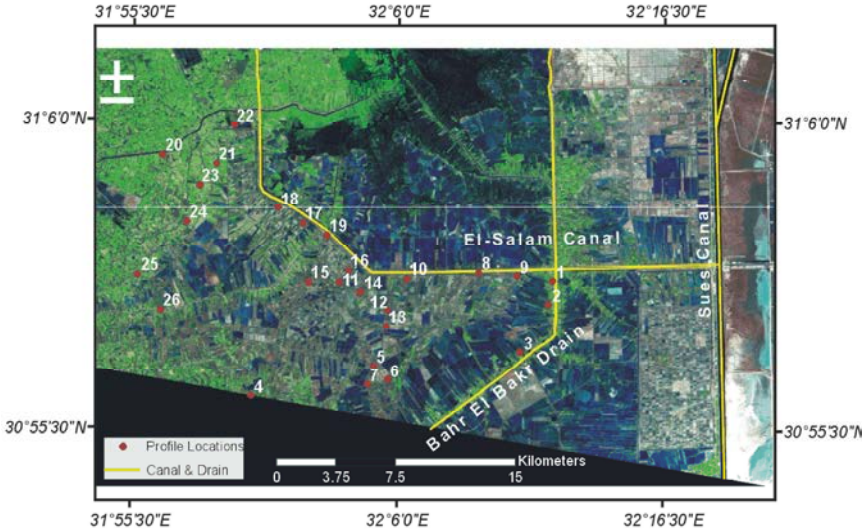

Fig. 1: Location of the experimental sites overlaid ETM+ image

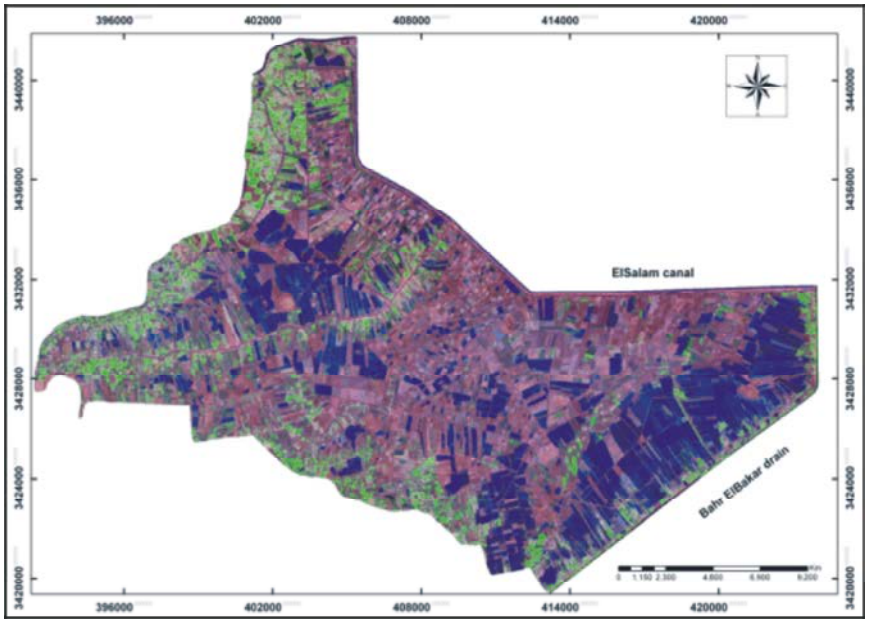

Fig. 2: Satellite image ETM+ of South El-Hussinia

Remote-Sensing Data: Landsat satellite image ETM+ data of the area, acquired in February, 2006 was processed using the ENVI® software (Fig. 2). The image was georeferenced by selecting ground control points from a (1:50,000) topographic map. This image was then georegistered and rectified to the UTM coordinate system (Zone 36) with WGS-1984 datum cartographic projection. Topographic map at scale (1:50,000) was scanned and the contour lines were digitized on screen. Linear interpolation follows to get digital elevation model (DEM) of the area with 30m ground resolution and spatial resolution to fit imagery data. A stereo image was generated (stereo anaglyph) using DEM and geomorphic interpretation was carried out using red-green glasses. Lines were delineated directly by on-screen digitizing. Maps were produced using Geographic Information System ArcGIS 9.3.

Spatial Prediction of Salinity Throughout the Region: Let the electrical conductivity observations be denoted $z(s_1)$, $z(s_2)$,…, $z(s_n)$, where s_i is a location vector and n the number of observations used for prediction purposes.

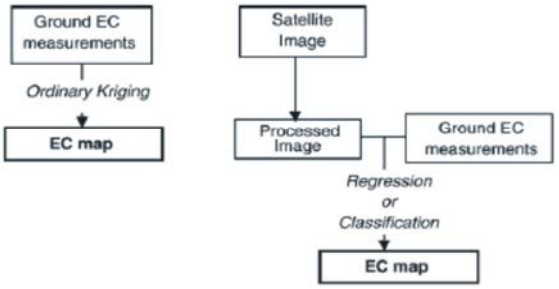

Fig. 3: Simplified diagrams of spatial estimation methods

Three types of prediction techniques had been used (Fig. 3) to estimate the $z^*(s_0)$ property at any new unvisited location (s_0) on the study area.

Ordinary Kriging (OK): Ordinary kriging with a spherical variogram was used as a basis of comparison with other methods, as predictions may only be derived from ground measurements:

$$z^*_{OK}(S_0) = \sum_{i=1}^{m} w_i(s_i) \times z(s_i)$$

where m is the number of neighbors considered and $w_i(s_i)$ are the weights derived from variogram fitting.

Classification (CL) and Simple Regression (SR): Remote sensing data were associated with soil measurements, by means of either simple regression (SR), which is the case with salinity or vegetation indices or assignment of EC values to classes (CL), which is the case for thematic data, such as land cover.

RESULTS

Remote-Sensing Data Processing

Image Classification and Geopedologic Analysis: The remote-sensing image was classified by a supervised method in order to obtain a land use map. The minimum distance criterion was applied in order to generate a mean classifier, wherein training data were used to estimate the class means; classification was then performed by assigning each pixel to the class of the nearest mean [18]. This classification method proved to be the most efficient for the present case. Training and validation sets of the supervised classification were created from both intrinsic knowledge of the environment and a land use inventory. In addition, information from previous pedological data, pre-existing land use maps and a digital elevation model, were employed. The ground observations were carried out over the entire Plain, including the area around El-Hussinia and the cultivated land.

According to the morphological description, climatic conditions, physical and chemical properties, the studied soils were classified, following the USDA Soil Taxonomy, as follows: 16 profiles as Typic Torrifluvents, 5 profiles as Aquic Torrifluvents, 4 profiles as Typic Haplosalids and a profile as Vertic Torrifluvents.

The resulting interpretation map for geomorphologic survey is shown in Fig. 4. Advantage of on-screen digitizing is that the interpretation lines are geocoded and no transformation is required to transfer the interpretation lines to base map. Eight classes were defined taking into account surface brightness as

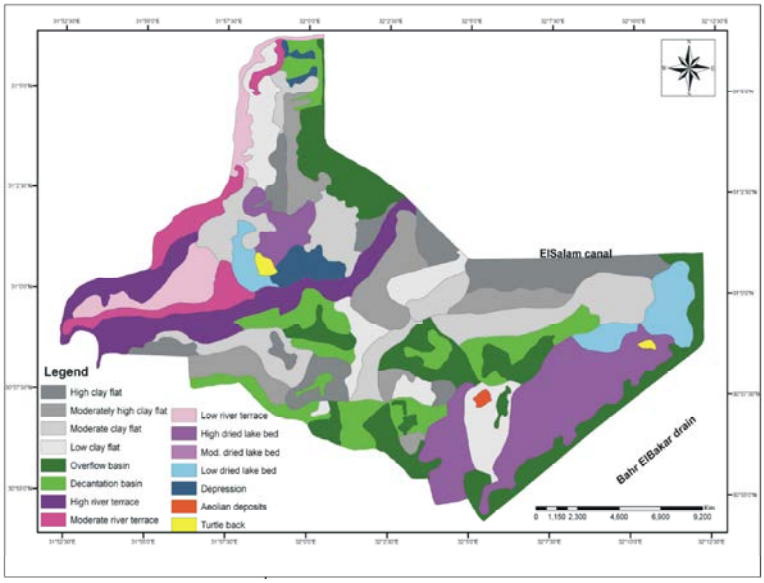

Fig. 4: Geomorphology map of South El-Hussinia area

Table 1: Some physical and chemical characteristics of the studied soils

							Particles Size Distribution %					
	Soil						----------					
Profile No.	depth (Cm)	pH	ECedS.m^{-1}	O.M	$CaCo_3$	Gypsum	Sand	Silt	Clay	Texture Classes	CECMeq.100g soil	ESP%
1	0-15	8.65	1.92	1.36	5.91	0.84	12.2	32.4	55.4	Clay	44.1	29.3
	15-40	8.61	1.72	1.45	6.26	0.45	14.1	33.5	52.4	Clay	45.1	33.9
	40-80	8.43	1.48	1.64	6.52	0.20	15.6	29.8	54.6	Clay	43.5	34.2
	80-120	8.42	3.69	1.89	6.75	0.22	13.9	32.2	52.9	Clay	40.4	36.5
	120-150	8.36	4.73	2.14	6.75	0.20	10.0	37.6	52.5	Clay	46.6	42.6
2	0-20	9.04	1.97	1.52	5.62	0.76	12.2	34.7	53.1	Clay	46.6	34.1
	20-45	8.78	4.25	1.77	6.13	0.52	11.2	33.2	55.6	Clay	46.7	31.8
	46-75	8.76	6.68	1.78	6.52	0.35	13.5	34.3	52.1	Clay	44.5	27.9
	75-105	8.67	8.69	1.83	6.64	0.21	13.3	32.9	52.7	Clay	43.2	25.6
	105-125	8.49	9.05	1.89	6.71	0.14	12.0	35.7	52.3	Clay	45.5	22.4
3	0-30	9.28	3.29	0.61	7.39	1.70	13.6	33.8	52.6	Clay	46.1	31.2
	30-55	8.55	5.69	0.75	6.82	1.36	11.7	36.8	51.5	Clay	41.8	29.3
	55-93	8.47	6.17	0.75	6.59	1.19	13.3	36.1	50.6	Clay	39.7	28.6
	93-115	8.42	7.48	0.89	5.18	0.49	16.2	40.3	43.4	Clay	42.6	25.4
	115-145	8.23	8.32	1.28	4.69	0.22	11.2	30.7	58.1	Clay	33.7	23.2
4	0-30	8.93	8.10	0.83	5.91	1.93	12.4	33.8	53.8	Clay	47.1	39.5
	30-55	8.86	9.79	0.84	5.77	0.79	14.2	38.4	47.5	Clay	42.4	38.5
	5-75	8.61	10.69	0.95	5.87	0.85	12.0	32.8	55.2	Clay	35.8	38.4
	65-110	8.46	11.58	1.92	6.19	0.57	13.6	37.1	49.2	Clay	40.3	35.8
	110-140	8.14	12.04	2.08	6.37	0.39	16.5	29.5	54.0	Clay	41.3	41.3
5	0-10	8.78	1.73	0.89	6.76	0.76	17.0	27.6	55.4	Clay	42.3	39.9
	10-35	8.55	1.42	1.06	6.86	0.55	15.0	34.7	50.3	Clay	36.6	40.1
	35-65	8.41	1.67	1.15	6.04	0.42	16.2	30.5	53.2	Clay	39.8	39.1
	65-100	8.35	2.40	1.64	4.68	0.39	13.8	38.9	47.3	Clay	33.1	44.5
6	0-25	9.12	4.65	0.81	6.98	0.54	14.8	35.3	49.9	Clay	35.0	29.3
	25-50	9.07	4.06	0.85	6.83	0.42	16.7	40.4	42.9	Clay	31.0	28.7
	50-75	8.78	4.11	0.87	6.06	0.31	10.6	34.6	54.8	Clay	43.5	32.4
	75-95	8.59	4.30	0.94	5.76	0.16	10.8	30.2	59.0	Clay	49.9	35.7
7	0-30	9.06	6.18	0.92	6.77	0.32	9.5	26.8	63.6	Clay	54.8	27.6
	30-50	8.88	6.96	1.29	6.80	0.26	22.3	38.1	39.6	Clay loam	33.3	41.6
	50-80	8.75	5.97	1.42	5.87	0.22	21.6	40.5	37.9	Clay loam	31.2	43.4
	80-100	8.48	5.25	1.49	5.59	0.22	13.9	29.0	57.1	Clay	41.0	49.9
8	0-20	9.17	3.59	0.58	7.05	0.84	15.2	39.9	44.9	Clay	44.7	49.4
	20-50	8.53	3.51	0.76	6.36	0.45	12.4	34.3	53.4	Clay	44.8	48.5
	50-85	8.47	3.19	0.85	6.02	0.44	14.5	26.6	58.8	Clay	42.7	41.4
	85-100	8.46	2.99	1.46	5.85	0.24	12.5	38.9	48.7	Clay	37.0	39.3
9	0-20	8.29	4.95	0.67	6.70	0.57	13.8	29.3	56.9	Clay	40.2	37.2
	20 - 40	8.36	4.52	0.73	6.20	0.36	21.8	30.4	47.8	Clay	37.5	36.4
	40-65	8.73	4.16	0.84	5.62	0.24	11.9	46.0	42.1	Clay	43.2	34.3
	65-100	8.76	3.91	1.60	5.49	0.18	14.2	49.4	36.4	Clay	40.1	28.9
	100-128	8.83	3.59	1.60	4.37	0.15	12.6	43.4	44.0	Clay	42.3	26.3
	130-160	8.37	4.48	1.12	5.32	0.15	10.6	33.5	55.9	Clay	45.7	35.9
10	0-20	8.42	4.98	0.49	4.67	0.26	21.1	42.3	36.6	Clay loam	35.7	59.3
	20-40	8.68	3.87	0.66	5.75	0.20	12.8	32.5	54.7	Clay	42.0	48.9
	40-80	8.71	2.7	0.81	4.86	0.18	15.2	37.1	47.7	Clay	59.6	45.8
	80-105	8.76	2.42	1.22	6.41	0.16	13.8	39.0	47.1	Clay	51.2	42.7

the main discriminating factor. The study area was geomorphologicly categorized into river terraces, clay flat and dried lake bed. These geomorphic units followed the high, moderate and low situated topography of the area, respectively. In addition, there were basin, depression and aeolian deposits whereas basin consisted of overflow basin and decantation one.

Characteristics of Soils Collected from El-Hussinia Plain

Soil General Characteristics: Data in Table (1) show some selected soil profiles with its physical and chemical properties of the studied soil. Values of the soil pH slightly increased with increasing soil depth. The values of soil pH ranged between 8.23 and 9.28 the studied soil profiles.

These variations in pH values between soil layers may be attributed to many factors such as increasing soluble Na^+, clay and $CaCO_3$ content. The most common cations in arid and semi-arid areas are calcium, magnesium and sodium. Each of these cations is base-forming, meaning that they contribute to an increased OH^- concentration in the soil solution and a decrease in H^+ concentration.

Some Physical Characteristics: There were many different soil texture types such as clay, clay-loam, sandy clay, sandy clay loam and sand. The majority of the soils in the region had mainly clay texture and clay loam texture type as shown in Figure 5.

Data illustrated in Figure 6 shows some physical properties of the studied soils. Values of clay content in the different sites increased with increasing soil depth. Such increases were observed clearly in the south eastern direction.

As expected, the surface layers of different soil profiles contained relatively high organic matter contents as they were compared with the sub-surface ones. On the other hand, total carbonate and gypsum contents showed little differences between different soil layers.

Chemical Characteristics

Soil pH, Salinity and Soluble Ions: Soil pH was distributed in an approximately normal fashion. Map distribution of soil pH values in the studied soil profiles are illustrated in Figure 7. Data showed that pH values of different soil layers ranged from 7.12 to the alkaline pH of 9.19 with the highest values in the upper layers. Values of the pH slightly increased with increasing soil depth. These variations in pH values may be attributed to many factors such as increasing soluble Na^+, clay and $CaCO_3$ contents.

The most common cations in arid and semi-arid areas are calcium, magnesium and sodium. Each of these cations is base-forming, meaning that they contribute to increase OH^- concentration in the soil solution and a decrease in H^+ concentration. Miller and Donahue [19] reported that soils with exchange complexes saturated with calcium, magnesium and sodium have a high base saturation and

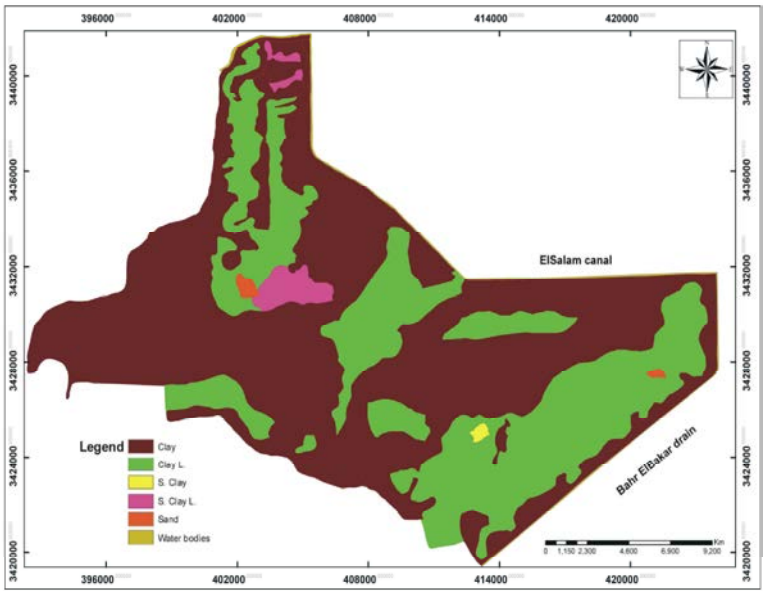

Fig. 5: Texture class map of southern El-Hussinia Area (Surface Area)

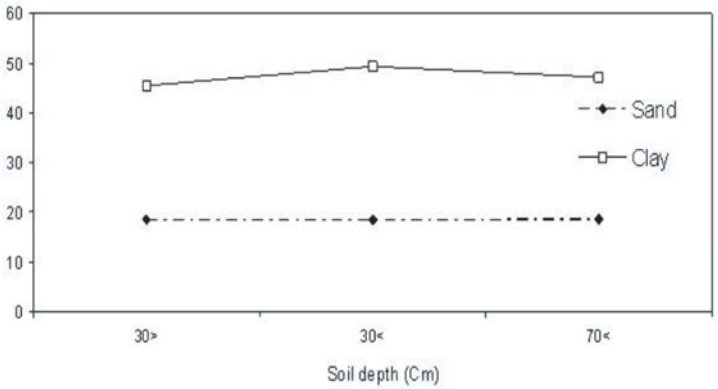

Fig. 6: Distribution of sand and clay values of the deferent soil sites with depth

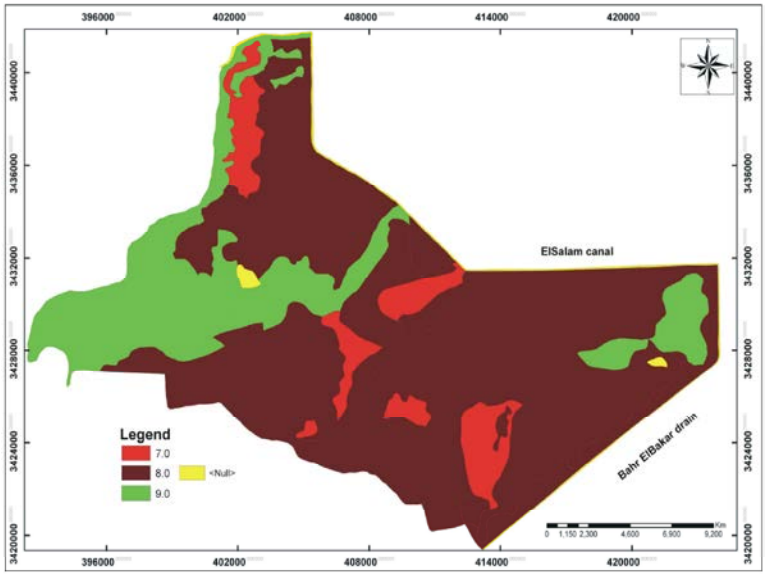

Fig. 7: Soil pH map of South El-Hussinia area (Surface layer)

typically high pH values. In addition, Qadir and Oster [20] showed a slight increase in soil pH as a result of applying saline irrigation water to soil; this increase was 4% in some soils.

DISCUSSION

Salinity Mapping by Means of Ordinary Kriging: The frequency distribution of EC (dS/cm) values in study area, exhibited abnormal distribution, which deemed *Ln* transformation prior to kriging. This gave a better fitting, however the problem of back transformation limiting its usability.

The mean experimental variogram was calculated up to a distance of 5000 m, this latter distance was maintained throughout the EC kriging estimation. A Spherical model fitted to the experimental variogram with a nugget

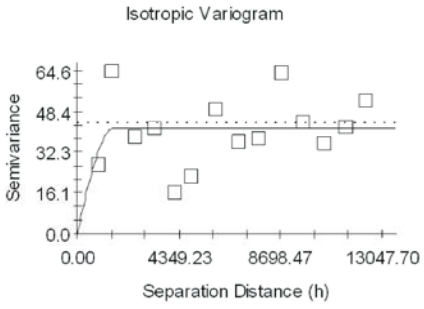

Fig. 8: EC mean experimental variogram

variance (Co) effect of 0.1 dS/m, a Sill (Co+C) of 41.72 dS/m and a range of 1540 m (Fig. 8).

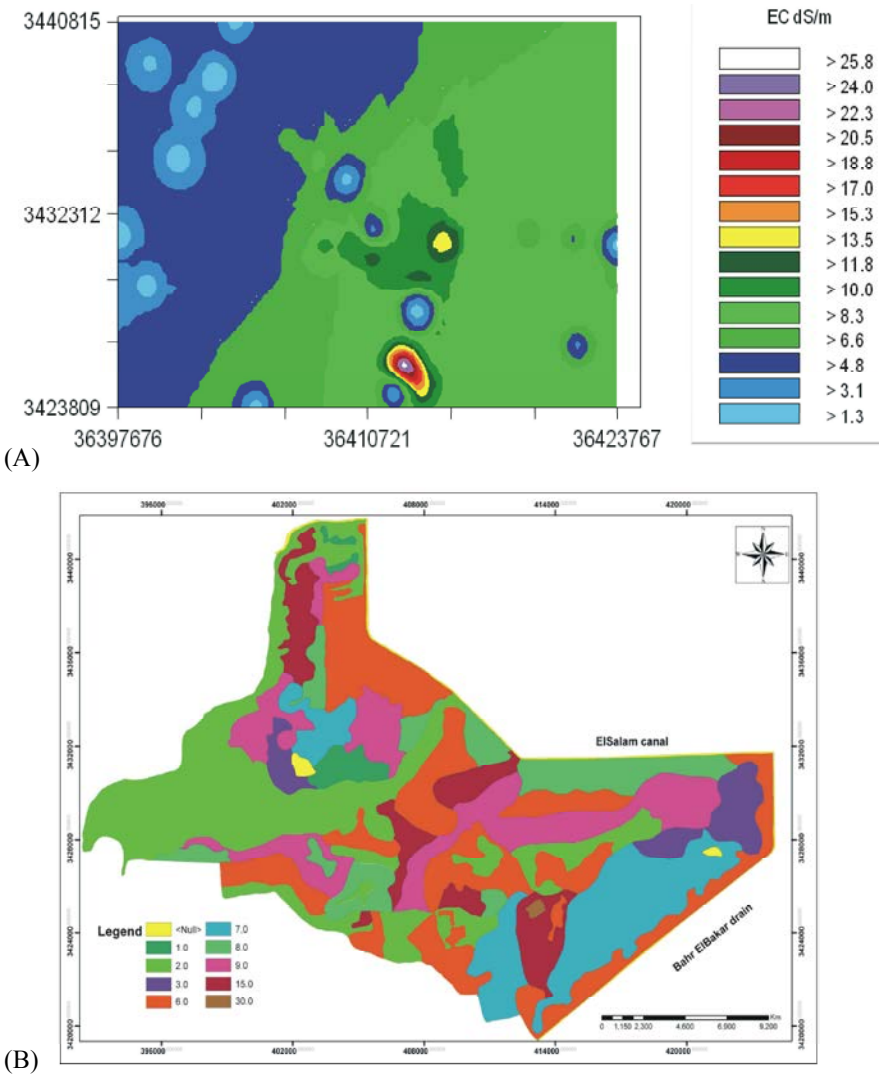

Fig. 9: Salinity maps spatial distribution of EC in South El-Hussinia (Surface layer)

The salinity map derived from ordinary kriging (Fig. 9) indicated that the most highly salt-affected areas were concentrated in the central lower part of the plain, particularly more close to Bahr El-Baher drain system (a closed depression). Electrical conductivity was systematically lower in the western part of the Plain than in neighboring areas, which can be explained by preferential drainage along the watercourse.

Several EC spatial structures, with distinct ranges and levels of variability, occurred in different small zones near by Bahr El-Baher drain, along with a very high nugget effect, which indicated a significant degree of short-range variability [21]. These effects exert a negative impact upon salinity estimation. The graph representing the scatter of points between all measured EC samples and EC estimated by OK (Fig. 10) indicated strong underestimation of high EC values. Validation results (OK) confirm this tendency to overestimate EC values below a mean value of 18 dS/m and to underestimate EC values above this limit. The regression coefficient calculated between measured and estimated EC values that represent a measure of the goodness of fit for the least-squares model describing the linear regression equation was 0.76 with a standard error of 0.67. This finding provided evidence of considerable smoothing of extreme values, as may be observed on the salinity map. Figure. 9 A & B illustrate the spatial distribution of salinity statutes pronounced by EC measurements in South El-Hussinia (Surface layer), derived from 2 mapping methods: ordinary kriging (OK) [22] © (part A) and classification (CL) (part B).

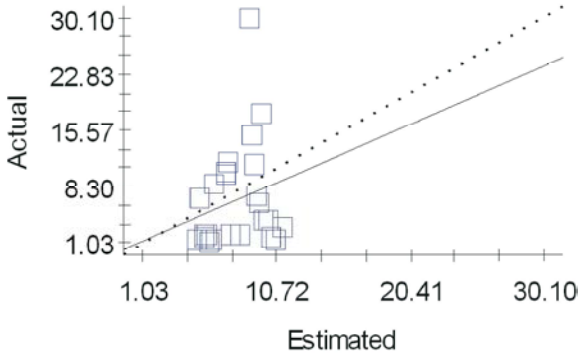

Fig. 10: Cross relationship between measured and estimated EC values (OK method)

Data Derived from Remote Sensing: The remote-sensing data are integrated in the form of a thematic and continuous raster image. The thematic map produced using this minimum distance classification has been presented in Fig. 9B. This map allowed discriminating the main land use type over the southern part of El-Hussinia Plain. The highly-saline soils of the plain were described by means of 3 primary classes [16]. They were corresponding to cultivated areas plus halophytic vegetation in the middle and eastern part of the study area (near Bahr El-Bakar drain). The cultivated areas that were located in the western part and along the main stream of El-Salam Canal were considered moderately to strongly saline. However, there were some small patches in the middle area are considered slightly saline soils. EC mean values of each class are presented in Fig. 11. The difference between EC classes means increases with EC level. The EC mean values difference between classes was higher by 10 (dS/m) for the Gaa areas saline soils and halophytic vegetation (ECN18 dS/m). However, for EC values under 18 (dS/m), which corresponds to cultivated areas and dark brown soils, the differences between classes amounted to less than 3 (dS/m).

Continuous data obtained from remote-sensing data has given rise to ten indices; these were compared with salinity values measured on the ground, by use of logarithmic fits (Fig. 9B).

Values of EC of the studied soil profiles decreased with increasing soil depth. The EC values reached in the upper layers (0-30cm) 1.23 fold that of the deepest one. It seems that slow downward movement of soluble salts in the heavy texture soils besides increasing water evaporation can cause salt accumulation in the upper layers [23]. This combines with the transpiration from the plant to concentrate salts in the root zone. Selem *et al*. [24] mentioned that, irrigation with drainage water generally seems to have a positive effect on salt

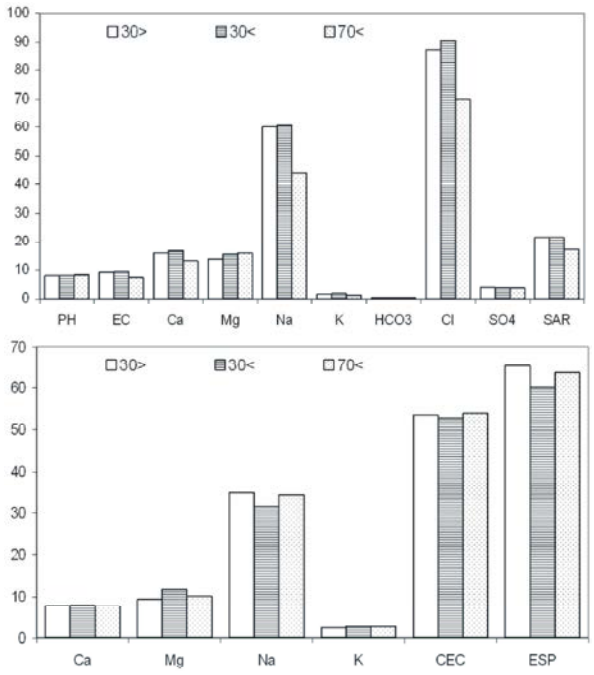

Fig. 11: Mean values of pH, EC, Soluble ions and SAR (up) – Exchangeable Cations, CEC and ESP (below) of the different soil sites

accumulation in soil profile and surface layers being the most affected. In addition, the salinity of soil solution is dependent on soil type, climate, water use and irrigation water characteristics.

Soil Sodicity Condition in El-Hussinia Plain: Soil sodicity is usually measured with one of two indices; one is the sodium absorption ratio (SAR) which give information on the comparative concentrations of Na^{+}, Ca^{2+} and Mg^{2+} in soil solution and the second one is the exchangeable sodium percentage (ESP), which measures the degree to which the exchange complex is saturated with sodium. The critical values for considering a soil sodic is 13 for SAR and 15 for ESP [25].

The obtained data in Fig. 11 indicated that SAR values extremely increased in the different soil profiles. So, standing from the recorded SAR values, the soil of El-Hussinia Plain area, that irrigated with low quality water, is considered sodic as its SAR was sharply higher than 13. Similarly, El-Sayed [26] reported that irrigating soil with drainage water seems to increase ESP of the clayey soil as a result of increasing SAR (Fig. 12).

Data presented in Fig. 11 show values of exchangeable cations and ESP of the tested soil profiles. The exchangeable Na^{+} was fairly higher, whereas Ca^{2+} was clearly lower one. It is worth to mention that

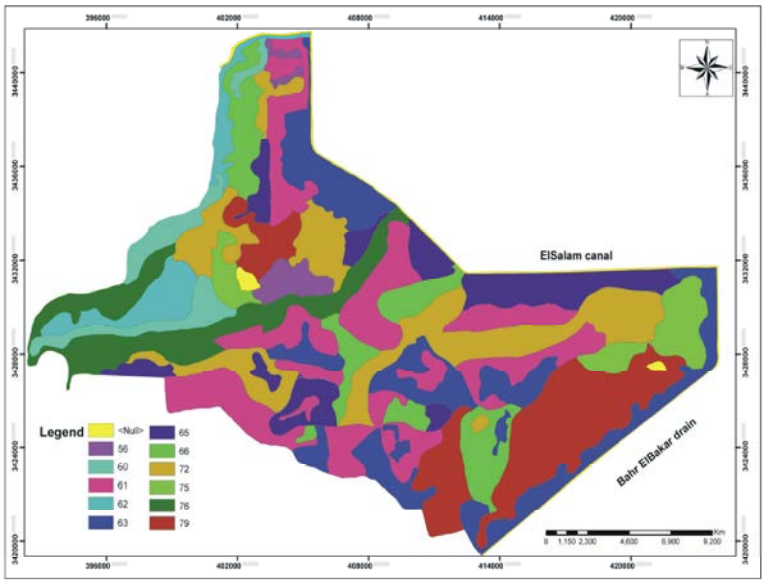

Fig. 12: ESP map of South El-Hussinia area (Surface layer)

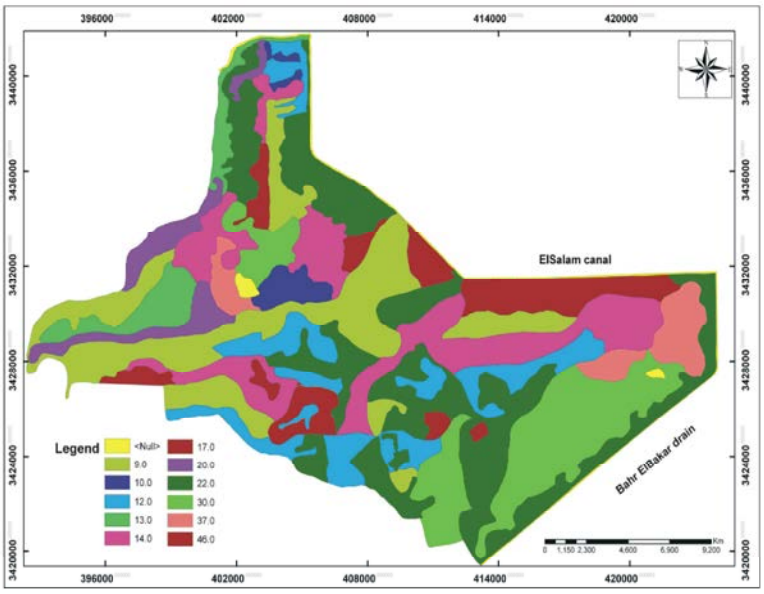

Fig. 13: SAR map of South El-Hussinia area (Surface layer)

the exchangeable cations in the different soil layers took similar order to that of the corresponding soluble cations of the same soil. Values of CEC of the investigated profiles in the different sites approximately were the same and they decreased with increasing soil depth (Fig. 13).

Comparison of the Two Applied Methods: The supervised classification method CL produced an estimated EC map (Fig. 9B) on which the main salinity areas had been correctly identified, in comparison with the OK method (Fig. 9A).This result was correlated with the choice of criteria used for selecting land cover classes, i.e., the coloration of vegetation and soil rightness.

Under conditions of the El-Hussinia Plain, this attribute is effectively correlated with various soil salinity levels. With the CL method, land use classes were associated with a mean EC value measured on the ground. By considering the mean for each land use class or each set of measured conductivity values, a smoothing of the values is necessarily being introduced by reducing the number of estimated EC values to the restricted number of classes.

Nevertheless, vegetation cover was not a suitable salinity indicator under the environmental conditions inherent in this study. As a general rule, the presence of vegetation corresponds to low salinity [27, 8]. During the summer period, non-saline soils correspond not only to cultivated and even irrigated areas, but also to bare soils or those covered with a thin layer of vegetation.

On the other hand, the salinity map obtained by ordinary kriging (OK) shows considerable smoothing of the EC classes, which alters the estimation of extreme values (b4 dS/m and N16 dS/m). In addition, the nugget effect, which represented nearly half of total variance, indicated a major local variability that exerted an impact on the quality of ordinary-kriging estimations.

In the case of low EC values, the surface areas obtained were smaller than these resulting from the CL method.

A comparison of the two maps derived from the two methods illustrated in figure 8 A and B show that for very high EC values (N25 dS/m), surface areas vary according to the two method chosen and decrease in the following order: OK>CL.

Using these two categories of methods as criteria for assessing the quality of estimations-ordinary kriging and remote sensing-based data-it would appear that the combined use of kriging and remote sensing markedly improves the accuracy of salinity mapping. The least effective estimations of salinity were those based on remote sensing data alone.

CONCLUSION

The produced maps allowed demonstrating the extent of salinisation in soils of the Lower El-Hussinia Plain. We have indeed observed a considerable extension in salinity, with 65% of the area being covered by saline soils (8 dS/m), of which 35% are composed of highly saline soils (16 dS/m). Non-saline soils (4 dS/m) make up only 20% of the soils found in this plain.

Although the salinity mapping using the classification (CL) method is less accurate than the OK method, nevertheless merits interest. Excluding cultivated areas from the classification and considering soil brightness for the determination of some classes could explain the relatively good result obtained from use of this method. Under the conditions experienced on the El-Hussinia Plain, the classes of moderate to low clay flat correspond to the highly-saline soils, but for 25 (dS/m), an underestimation of EC may occur. The surface areas are classified only ten mean values of EC corresponding to the land use classes inferred from the satellite image.

These results allowed envisaging new prospects in the field of spatial-temporal salinity monitoring. We must first analyze the sampling protocol using a minimum number of samples, in which exogenous spatial data from remote-sensing images or other existing information sources are associated with ground-based measurements. Mention could be made, for example, of stratified sampling within the context of saline soils. Such an approach should lead to increased accuracy both in the analysis of existing data once satellite images are available and in salinity monitoring with fewer restrictive ground measurements in order to achieve acceptable mapping accuracy.

In conclusion, it remains necessary to apply these approaches under different conditions and on various sites in order to increase the robustness of the methods developed

REFERENCES

1. El-Degwi, A.M.M., F.M. Ewida and S.M. Gawad, 2003, Estimating bod pollution rates along El-Salam Canal using monitored water quality data. Presented at the 9th International Drainage Workshop, September 10-13, 2003, Utrecht, The Netherlands. Paper No. 050.
2. Ferreyra, R.A., H.P. Apezteguia, R. Sereno and J.W. Jones, 2002. Reduction of soil water spatial sampling density using scaled semi-variograms and simulated annealing. Geoderma, 110: 265-289.
3. Li, Y., Z. Shi, C.F. Wu, H.X. Li and F. Li, 2007 Improved prediction and reduction of sampling density for soil salinity by different geostatistical methods. Agricultural Sciences in China, 6: 832-841.
4. Emery, X. and J.M. Ortiz, 2007. Weighted sample variograms as a tool to better assess the spatial variability of soil properties. Geoderma, 140: 81-89.
5. Boken, V.K., G. Hoogenboom, J.E. Hook, D.L. Thomas, L.C. Guerra and K.A. Harrison, 2004. Agricultural water use estimation using geospatial modeling and a geographic information system. Agric. Water Manage., 67: 85-199.
6. Robinson, T.P. and G.M. Metternicht, 2006. Testing the performance of spatial interpolation techniques for mapping soil properties. Computer and Electronics in Agriculture, 50: 97-108.
7. **Missing**
8. Sokoti, S., M. Mahdian, S.H. Mahmoodi and A. Ghahramani, 2007. Comparison the applicability of some geostatistical methods to predict soil salinity, a case study of Urmia plain. J. Pajuhesh and Sazandegi, 74(1): 90-98.

9. Darwish, K.H.M., M.M. Kotb and R.R. Ali, 2007 Estimating spatial variability of soil salinity using cokriging in Bahariya oasis, Egypt. Egypt. J. Soil. Sci., 47(2): 99-116.
10. Florinsky, I.V., R.G. Eilers and G.W. Lelyk, 2000. Prediction of soil salinity risk by digital terrain modelling in the Canadian prairies. Canadian Journal of Soil Science, 80: 455-463.
11. Metternicht, G., 2001. Assessing temporal and spatial changes of salinity using fuzzy logic, remote sensing and GIS. Foundations of an expert system. Ecological Modelling, 144: 163-179.
12. Navarro-Pedreño, J., M.M. Jordan, I. Meléndez-Pastor, J. Gómez, P. Juan and J. Mateu, 2007. Estimation of soil salinity in semi-arid land using a geostatistical model. Land Degradation and Development, 18: 339-353.
13. Juan, P., J. Mateu, M.M. Jordan, J. Mataix-Solera, I. Meléndez-Pastor and J. Navarro-Pedreño, 2011. Geostatistical methods to identify and map spatial variations of soil salinity. Journal of Geochemical Exploration, 108: 62-72.
14. Said, R., 1993. The River Nile geology and hydrology and utilization. Britain Pergmon Press, Oxford, pp: 320.
15. Ayyad, M.A., M. Abdel-Razik and S. Mehannas, 1983. Climatic and vegetational gradients in the Mediterranean desert of Egypt. Pre-report of the Mediterranean Bioclimatic Symposium, Montpellier, France, 18-21 May; 1-14.
16. FAO, 2006 Guidelines for Soil Description. 4th edition. Roma: FAO.
17. Usda Soil Conservation Service, 2010. Keys to Soil Taxonomy by Soil Survey Staff. Eleventh Edition, USDA Agriculture Handbook, 436. Washington, D.C.
18. Richards, J.A. and X. Jia, 1999. Remote Sensing Digital Image Analysis: An Introduction. Springer-Verlag, Berlin Heidelberg.
19. Miller, R.W. and R.L. Donahue, 1995. Soils in our Environment, Seventh Edition. Prudence Hall, Englewood, Cliffs, NJ., pp: 323.
20. Qadir, M. and J.D. Oster, 2004. Crop and irrigation management strategies for saline-sodic soils and waters aimed at environmentally sustainable agriculture. Science of the Total Environment, 323: 1-19.
21. Walter, C.H., A.B. McBratney, A. Douaoui and B. Minasny, 2001. Spatial prediction of topsoil salinity in the Cheliff Valley, Algeria, using local ordinary kriging with local variograms versus whole-area variogram. Aust. J. Soil Res., 39: 259-272.
22. Gamma Design Software LLC (1989-2005) © All Rights Reserved.
23. Mahida, U.N., 1983. Water Pollution and Disposal of Waste Water on Land, pp 1-5, 7-26 Mahida U N (ed.), New Delhi, pp: 225.
24. Selem, M.M.I., A.A. El-Gayar, R.M. El-Awady and H. Abd El-Gawad, 1989. Effect of irrigation with drainage water on some physical properties of soils. Annals of Agric Sci. Moshtohor, Zagazeg Uni., 27(4): 2533-2545.
25. Brady, N.C. and R.R. Weil, 1996. The nature and properties of soil. Prentice-Hall, International, Inc. London.
26. El-Sayed, A.H., 1990. Effect of drainage water quality on soil and plant. M.Sc. Thesis, Fac. of Agric. Ain Shams Univ. Egypt.
27. Manière, R., E. Bassisty, J.C. Celles and S. Melzi , 1993. Utilisation de la télédétection spatiale (données XS de Spot) pour la cartographie de l'occupation du sol en zones arides méditerranéennes: exemple d'Aïn Oussera (Algérie). Cah. ORSTOM, Ser. Pédol. XXVIII 1: 67-80.
28. Rahman, S., G.F. Vance and L. Munn, 1994. Detecting salinity and soil nutrient deficiencies using Spot satellite data. Soil Sci., 158(1): 31-39.